Silicon-on-Insulator microring resonator for sensitive and label-free biosensing

Katrien De Vos[1*], Irene Bartolozzi[2], Etienne Schacht[2], Peter Bienstman[1], Roel Baets[1]

[1]*Photonics Research Group, Dept. of Information Technology, Ghent University – IMEC*
Sint-Pietersnieuwstraat 41, 9000 Gent, Belgium
[2]*Polymer Chemistry and Biomaterials Research Group, Ghent University*
Krijgslaan 281 (S4 Bis), 9000 Gent, Belgium
[*] *Katrien.Devos@intec.UGent.be*

Abstract: Label-free biosensors attempt to overcome the stability and reliability problems of biosensors relying on the detection of labeled molecules. We propose a label-free biosensor based on microring cavities in Silicon-on-Insulator (SOI) that fits in an area below $10x10\mu m^2$. The resonance wavelength shift that occurs when the surroundings of a cavity is changed, is used for sensing. While theoretically the performance for bulk refractive index changes is moderate (10^{-5}), this device performs outstanding in terms of absolute molecular mass sensing (theoretical sensitivity of 1fg molecular mass) thanks to its extremely small dimensions. We use the avidin/biotin high affinity couple to demonstrate good repeatability and detection of protein concentrations down to 10ng/ml. Fabrication with Deep UV lithography allows for cheap mass production and integration with electronic functions for complete lab-on-chip devices.

OCIS codes: (130.3120) Integrated Optics Devices; (130.6010) Sensors; (230.5750) Resonators

References and links

1. J. Homola, "Present and Future of Surface Plasmon Resonance Biosensors," Anal. Bioanal. Chem. **377**, 528-539 (2003).
2. P.P.P. Debackere, S. Scheerlinck, P. Bienstman, R. Baets, Surface Plasmon Interferometer in Silicon-on-Insulator: novel concept for an integrated biosensor," Opt. Express **14**, 7063-7072 (2006).
3. D. Hradetzky, C. Mueller, H. Reinecke, "Interferometric Label-free Biomolecular Detection System," J. Opt. A: Pure Appl. Opt. **8**, S360-S364 (2006).
4. A. Ymeti, J. Greve, P.V. Lambeck, T. Wink, S.W.F.M. van Hövell, T.A.M. Beumer, R.R. Wijn, R.G. Heideman, V. Subramaniam, J.S. Kanger, "Fast, ultrasensitive virus detection using a Young interferometer sensor," Nano Lett. **7**, 394-397 (2007).
5. A. Ksendzov, Y. Lin, "Integrated Optics Ring-resonator Sensors for Protein Detection," Opt. Lett. **30**, 3344-3346 (2005).
6. C-Y. Chao, W. Fung, L.J. Guo, "Polymer Microring Resonators for Biochemical Sensing Applications," IEEE J. Sel. Top. Quantum Electron. **12**, 134-142 (2006).
7. A. Yalçin, K.C. Popat, J.C. Aldridge, T.A Desai, J. Hryniewicz, N. Chbouki, B.E. Little, O. King, V. Van, S. Chu, D. Gill, M. Anthes-Washburn, M.S. Ünlü, B.B. Goldberg, "Optical Sensing of Biomolecules Using Microring Resonators," IEEE J. Sel. Top. Quantum Electron. **12**, 148-155 (2006).
8. *Biomedical Photonics Handbook*, edited by Vo-Dinh T. (CRC Press LLC, Boca Raton, 2003).
9. J. Vörös, "The Density and Refractive Index of Adsorbing Protein Layers," Biophys. J. **87**, 553-561 (2004).
10. C.C. Striemer, T.R. Gaborski, J.L. McGrath, F.M. Fauchet, "Charge- and size-based separation of macromolecules using ultrathin silicon membranes," Nature **445**, 749-753 (2007).
11. W. Bogaerts, R. Baets, P. Dumon, V. Wiaux, S. Beckx, D. Taillaert, B. Luyssaert, J. Van Campenhout, P. Bienstman, D. Van Thourhout, "Nanophotonic Waveguides in Silicon-on-Insulator Fabricated with CMOS Technology," J. Lightwave Technol. **23**, 401-412 (2005).
12. *Handbook of Chemistry and Physics*, edited by D.R. Lyde, (CRC press, London, 1997-1998)
13. F. Zhang, M.P. Srinivasan, "Self-assembly molecular films of aminosilanes and their immobilization capacities," Langmuir **20**, 2309-2314 (2004).

#81541 - $15.00 USD Received 27 Mar 2007; revised 30 May 2007; accepted 30 May 2007; published 6 Jun 2007

14. R. Ince, R. Narayanaswamy, "Analysis of the performance of interferometry, surface plasmon resonance and luminescence as biosensors and chemosensors," Analytica Chimica Acta **569**, 1-20 (2006).

1. Introduction

Optical label-free biosensors for protein detection attempt to overcome the drawbacks of commercialized microarrays, which rely on the detection of labeled molecules. This intermediate labeling step however complicates the sample preparation and detection process, the label can alter the molecule's binding properties and therefore decrease detection reliability. Direct detection of biomolecules enables the monitoring of the dynamics of molecular reactions, quantitative concentration measurements, and determination of affinity constants. When direct biosensors can be integrated on a chip, high throughput screening of biomolecular interactions in microarrays becomes possible without an intermediate labeling step. Different approaches for integrated optical biosensors based on Surface Plasmon Resonances (SPR) [1,2], interferometers [3,4] and resonant cavities [5-7] are previously reported. We propose a Silicon-on-Insulator biosensor based on microring cavities, fabricated with standard CMOS processing, in particular deep ultraviolet lithography [12], allowing for cheap mass fabrication and integration with electronics and easily extendable to a multiarray biosensor with thousands of sensing spots for real lab-on-chip devices. The biosensor enables quantitative and real time measurements, fast sample preparation and detection of extremely low analyte quantities. SOI offers a high refractive index contrast suitable for the fabrication of nanophotonic circuits including micron- and submicron sized optical cavities of very high quality. The enhanced light-matter interaction in a cavity increases the sensitivity while keeping the sensor's dimensions small. Integrated in a microfluidic setup thousands of cavities can be lined up in arrays for multiparameter sensing within a few square millimeters.

Using telecom wavelengths for biosensing allows the reuse of standardized telecom equipment. The absorption of light in the near infrared is dominated by water absorption, since biomolecules are transparent at wavelengths longer than 500nm [8]. Since there is a dip in the water absorption spectrum at 1550nm, we believe that 1550nm is a suitable wavelength for biosensing purposes. Considering the small dimensions of the cavity the disturbance of the resonance due to water absorption is negligible.

Biosensing based on semiconductor materials requires chemical modification of the silicon surface in order to provide a suitable biointerface. The surface modification both provides the immobilization of the biomolecule in its most active conformation and prevents nonspecific protein adsorption, which can affect the sensitivity and specificity of the biosensor.

The rest of the paper is structured as follows. Paragraph 2 covers the working principle, sensitivity and fabrication of the device. Paragraphs 3, 4 and 5 discuss the characterization of the device for bulk refractive index sensing and surface sensing.

2. Biosensing with SOI microring resonators: theory and fabrication

2.1 Sensing principle and sensitivity

We designed a microring cavity in an add-drop filter configuration (Fig. 1(a)). The ring supports modes that resonate at a wavelength $\lambda_{resonance}$ for which:

$$\lambda_{resonance} = \frac{L}{m} n_{eff} \tag{1}$$

L is the round trip length and m is the cavity mode order (=1,2...). The resonance results in a sharp dip in the transmission (Fig. 1(b)). A change of the refractive index of the cavity's

#81541 - $15.00 USD Received 27 Mar 2007; revised 30 May 2007; accepted 30 May 2007; published 6 Jun 2007

environment shifts the resonance spectrum, which can be monitored both by scanning the wavelength and by measuring the intensity profile at one well chosen wavelength.

When discussing sensitivity, there are two figures of merit for it: sensitivity for bulk refractive index changes and sensitivity for homogenous covering of the surface with a molecular layer of mass $M=\rho\ S\ t$, ρ being the mass density of the molecular layer, S the sensing area and t the thickness of the layer. From Eq. (1) we obtain:

$$\Delta n_{\min} = \frac{m}{L}\left(\frac{\partial n_{eff}}{\partial n_{bulk}}\right)^{-1} \Delta\lambda_{\min} \tag{2}$$

$$\Delta M_{\min} = \rho S \frac{m}{L}\left(\frac{\partial n_{eff}}{\partial t}\right)^{-1} \Delta\lambda_{\min} \tag{3}$$

When the resonance used in the measurement is in a given wavelength band (1550 nm in our case), the cavity mode order m scales with the cavity length L so the ratio m/L is constant and independent of cavity length. Therefore the minimal detectable bulk refractive index change Δn_{min} is independent of the microring's radius. But the minimal detectable protein mass ΔM_{min} does scale with the area. When it decreases, fewer molecules are needed to cover the sensing area while the resonance shift will not be influenced negatively by the decreasing round trip length. This allows for the detection of an extremely small mass of biomolecules. Simulation of $\partial n_{eff} / \partial t$ for a curved waveguide with radius 5 μm results in 0.3/pm –side wall binding taken in consideration– while ρ is approximately 1.33g/cm^3 [9] and the ring's surface area is 21,8 μm^2. For a minimal detectable wavelength shift of 5 μm – a realistic value for our device –a minimal mass of 0.7fg can be detected. Since biomolecules are provided in liquids such as blood or serum one has to find an elegant way to bring molecules at the sensing surface in an acceptable time. Recently a solution for this fluidic issue has been discussed in [10].

In order to minimize the smallest detectable wavelength shift $\Delta\lambda_{min}$, high Q cavities and a low noise detection system is required. A high Q-factor results in narrow spectral peaks: $Q = \lambda_{resonance} / \Delta\lambda_{3dB}$. A number of parameters determine the cavity's Q-factor. Firstly, reduced optical losses enhance the Q-factor. Secondly, a larger gap between the input/output waveguides and the ring waveguide reduces the coupling coefficient and therefore the cavity losses, although this increases the throughput attenuation at the same time. In our design a racetrack shape is used in order to have more control over the coupling coefficient. Lateral waveguide coupling is used in order to minimize the required fabrication steps. Finally, smaller radii will increase bend losses but reduce scattering losses because of decreasing round trip length. An optimum for the radius can be found, although in our fabricated devices scattering losses are dominant, so the radius of 5μm is not the lower limit yet. For waveguide dimensions of 500nm x 220nm and a radius of 5 μm, Q-factors over 20,000 and a Free Spectral Range of 15nm are easily achievable with standard CMOS processes and optimized design. This results in a 3dB peak width of the microring resonance of about 75pm.

2.2 Fabrication

The SOI material system highly reduces the dimensions of the devices compared to traditional passive photonic components. Thanks to the high refractive index contrast, the waveguide core is largely reduced in size to keep the waveguide single mode and total internal reflection guiding is guaranteed for very small bend radii. A consequence of the high lateral index contrast is that the waveguides become more sensitive to scattering at roughness on the core-cladding interface. To this end high-quality and high-resolution fabrication tools are required. Deep ultraviolet (UV) lithography, the technology used for advanced complementary metal-oxide-semiconductor (CMOS) fabrication offers both the required resolution and the throughput needed for commercial applications. Standard CMOS fabrication processes were

#81541 - $15.00 USD Received 27 Mar 2007; revised 30 May 2007; accepted 30 May 2007; published 6 Jun 2007

adopted to improve their capability for fabricating photonic nanostructures. This was previously reported in [11].

3. Measurement setup

A schematic drawing of the proof-of-principle measurement setup is given in Fig. 1(c). The optical chip is placed on a temperature stabilized chuck. A flow cell is mounted on the chip, connected through tubings with a peristaltic pump in order to switch easily between the liquids flown over the sensor. Measurements are done statically i.e. at zero flow rate; we make sure we measure when all reactions have reached equilibrium.

Optical fibers are vertically coupled to the in- and output integrated waveguides through grating couplers [11]. This allows for easy coupling with high alignment tolerances. Light coming from a tunable laser, passes the integrated circuit and is detected with a photodetector.

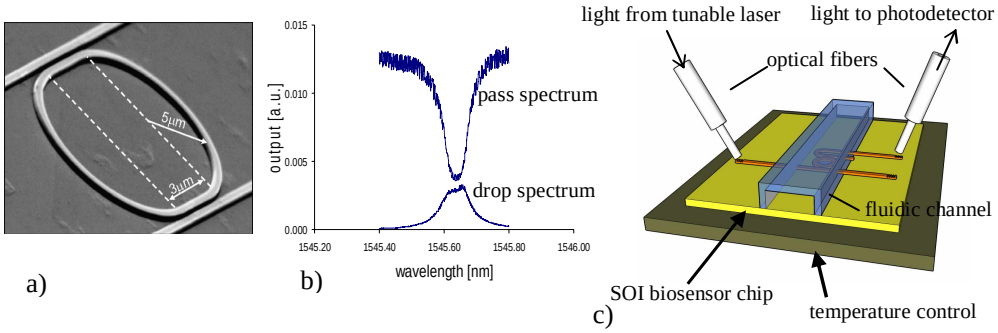

Fig. 1. a) SEM picture of a microring cavity, b) measured spectra, c) measurement setup.

4. Bulk refractive index sensing

Liquids with varying refractive indices (water with different sodium chloride concentrations) are flown across the ring resonator in order to characterize the sensor for bulk refractive index sensitivity. No surface chemistry was carried out, so the refractive index is homogenously changed above the ring resonator. At 20°C the refractive index of an aqueous solution of NaCl varies with 0,0018 RIU (Refractive Index Units) per mass % [12]. Fig. 2 shows a linear shift of the resonance wavelength with increasing salt concentration of 70nm/RIU, the shifts are determined after Lorentzian fitting. All measurements are done three times to prove repeatability. The linear fit is depicted with mean wavelength shift values and weighted variance error bars. The variations are very small, proving a very high refractive index sensor's stability. A shift of one fifteenth of the peak width is easily measurable, so a minimal detectable wavelength shift of 5pm corresponds with a minimal detectable refractive index shift of 10^{-5} RIU.

5. Protein interaction sensing

In the present work we used the avidin/biotin system, which has a high affinity constant ($K_a = 10^{15} M^{-1}$) and therefore gives a very specific and stable interaction, as a model of biomolecular ligand/receptor interaction.

5.1 Surface functionalization

Silanization of the surface by condensation of surface silanols with functionalized silanes can be used to provide a suitable biointerface between the transducer element and the biological medium. Surfaces were modified according to the following procedures [13]. Toluene and N,N-dimethylformamide (DMF) were distilled before use. 3-aminopropylsilane (APTES) and

#81541 - $15.00 USD Received 27 Mar 2007; revised 30 May 2007; accepted 30 May 2007; published 6 Jun 2007

succinimidyl-6(biotinamido)hexanoate (E,Z link-NHS-LC-Biotin) were used as received. Surfaces were cleaned and oxidized in Piranha solution (H_2SO_4:H_2O_2, 7:3) at 50°C for 1 hr, in order to expose hydroxyl groups on the surface. Cleaned and oxidized silicon surfaces were silanized by immersion in 1% dry toluene solution of APTES for 4 hours The substrates were then rinsed thoroughly with toluene and DI-H_2O. Aminosilanized surfaces (Si-APTES) were then immersed in 2ml Phosphate Buffer Solution (PBS) pH 7.5 and 100μl of E,Z link-NHS-LC-Biotin in DMF (1mg/ml) was added. The reaction was carried out for 3 hours at room temperature. Surfaces were rinsed with PBS and DI-H_2O.

5.2 Surface characterization

Flat Si surfaces were characterized after each modification step by static contact angle (OCA 20 from Dataphysics, distributed by Benelux Instrument), AFM (Nanoscoop III, Digital) and ellipsometry (Applied Materials Ellipsometer II, λ=632.8 nm and α=70°).

Contact angle measurements show an increasing hydrophobicity when the surface is coated using increasing APTES concentrations (0.2% to 2% correspond with 65° to 75°). This indicates that increasing the APTES concentration results in a formation of multilayers and the amino groups can also intramolecularly interact with the underlying layers of silanes. AFM measurements confirmed the formation of multilayers by showing a slightly increased roughness and globular nuclei size at high APTES concentrations.

Ellipsometric measurements are used to determine the thickness of the layer after each modification step. The refractive index for all the surface layers is assumed to be 1.45, in agreement with literature stated values [9]. After silanization, the thickness increased from 2.8nm of the plain silicon surface, to 9.5nm. Biotin immobilization did not significantly affect the thickness, but after incubation of the biotinylated surface with avidin followed by extensive rinsing, the thickness increased to 14.9nm, indicating the immobilization of the large avidin molecules on the surface. On the contrary, when the aminosilanized surface - not biotinylated - was exposed to avidin solution, no significant increase in thickness was observed, suggesting that no significant interaction between avidin and the surface took place. Comparing the two experiments proves the presence of biotin on the surface.

5.3 Surface sensing of specific protein interaction

We compare the resonance wavelength of the cavity immersed in PBS, before and after being in contact with avidin solution (avidin in PBS). Redundant avidin molecules are rinsed thoroughly with PBS, so no bulk refractive index changes are involved. The evolution of the wavelength shift for different avidin concentrations compared to the reference PBS resonance wavelength is shown in Fig. 3. All measurements are performed with at least 3 different samples, and error bars are indicated. For avidin concentrations above 10μg/ml the surface is fully covered, the resonance wavelength shift saturates. This is another proof that we detect a surface modification and not a bulk liquid modification, like in figure 2. For smaller avidin concentrations we see a smaller wavelength shift which allows us to quantify the avidin concentration. The estimated lowest detectable concentration, for a minimal detectable wavelength shift of 5pm, is 10ng/ml. This compares well with commercially available label-free protein detection methods [14].

Specificity is an important feature of a label-free biosensor. To prove that the sensor is sensitive to specificity, Bovine Serum Albumin (BSA), a protein with similar molecular weight to avidin but with low affinity to biotin, is brought into contact with the biotin layer. In graph 4 we clearly see a lower interaction.

Measuring the output intensity at one wavelength is used for real time interaction detection. Graph 5 shows real time measurements for 10ng/ml and 50ng/ml avidin concentrations. The dip in the curves is a transient phenomenon, due to the switching of the pump. The rise time is due to both the protein interaction rate and the mixing in the flow cell. In order to eliminate the latter effect a microfluidic setup with a constant flow rate will be used in future experiments in order to determine protein affinity constants and binding rates.

#81541 - $15.00 USD Received 27 Mar 2007; revised 30 May 2007; accepted 30 May 2007; published 6 Jun 2007

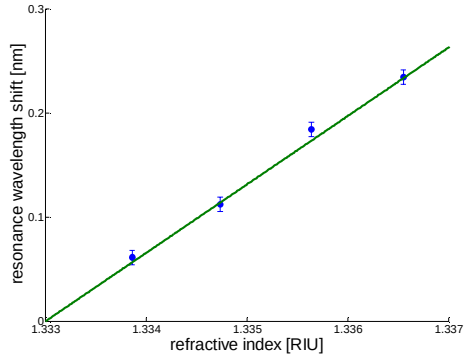

Fig. 2. Resonance wavelength shift versus bulk refractive index change.

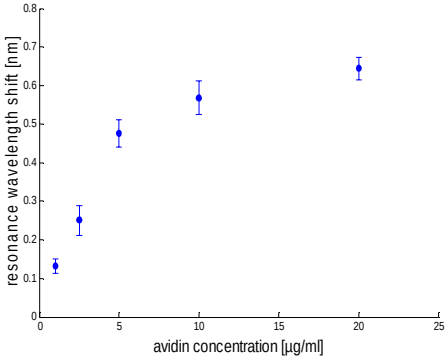

Fig. 3. Resonance wavelength shift corresponding to different avidin concentrations for quantitative molecular detection.

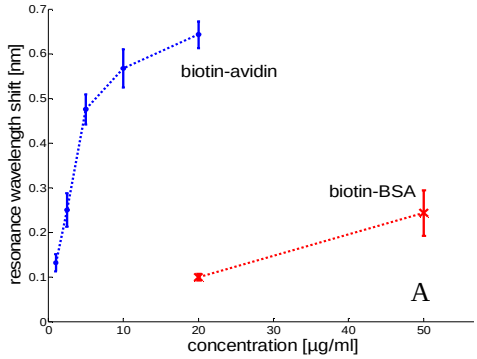

Fig. 4. Non-specific binding tests to show a lower output for biotin/BSA interactions.

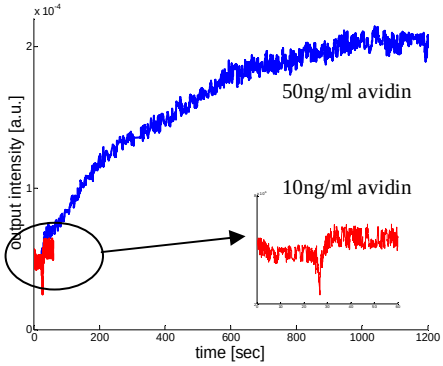

Fig. 5. Real time interaction measurements for different avidin concentrations.

6. Conclusions

We have demonstrated a highly miniaturized optical label-free biosensor based on a Silicon-on-Insulator microring cavity. Its high Q-factor and its extreme small size – radius of 5 micron – allow this device to sense low amounts of analyte (coverage of 0.7 fg molecular layer). The mass fabrication method by deep-UV lithography makes the devices very suitable for high throughput biosensing in commercial applications. The refractive index sensitivity is 10^{-5} independent of the microring's radius. The silicon surface was modified for biosensing purposes in a two step reaction consisting of aminosilanization and biotin covalent binding. Measurements reveal proper operation of the device, being able to detect protein concentrations down to 10ng/ml for the large avidin molecule, which compares favorably with commercial biosensing applications.

Acknowledgments

This work was partially funded by Ghent University through the GOA project B/05958/01. K. De Vos thanks the Flemish Institute for the Promotion of Innovation through Science and Technology (IWT) for a specialization grant. P. Bienstman acknowledges the Flemish Fund for Scientific Research (FWO-Vlaanderen) for a postdoctoral fellowship.

#81541 - $15.00 USD Received 27 Mar 2007; revised 30 May 2007; accepted 30 May 2007; published 6 Jun 2007